

See discussions, stats, and author profiles for this publication at: <https://www.researchgate.net/publication/266373201>

Experimental and modeling study on the high-temperature oxidation of Ammonia and related NOx chemistry

ARTICLE *in* COMBUSTION AND FLAME · OCTOBER 2014

Impact Factor: 3.08 · DOI: 10.1016/j.combustflame.2014.08.022

CITATION

1

READS

64

2 AUTHORS, INCLUDING:



Olivier Mathieu

Texas A&M University

40 PUBLICATIONS 275 CITATIONS

SEE PROFILE



Contents lists available at ScienceDirect

Combustion and Flame

journal homepage: www.elsevier.com/locate/combustflame

Experimental and modeling study on the high-temperature oxidation of Ammonia and related NOx chemistry

Olivier Mathieu*, Eric L. Petersen

Department of Mechanical Engineering, Texas A&M University, College Station, TX 77843, USA

ARTICLE INFO

Article history:

Received 22 July 2014

Received in revised form 27 August 2014

Accepted 27 August 2014

Available online xxxx

Keywords:

Ammonia

Ignition delay time

Shock tube

High pressure

Detailed kinetics modeling

ABSTRACT

Ammonia oxidation and ignition delay time measurements for pressures above 10 atm are scarce. In addition, NH₃ is known to adsorb on stainless steel, so measurement results could be in question if wall passivation is not employed for apparatuses utilizing steel. To overcome these measurement difficulties and overall lack of high-pressure data for ammonia, new and methodical ignition delay time measurements have been performed behind reflected shock waves over a wide range of temperatures (1560–2455 K), pressures (around 1.4, 11, and 30 atm) and equivalence ratios (0.5, 1.0, and 2.0) for mixtures of ammonia highly diluted in Ar (98–99%). The new set of data from the present study was compared to several models from the literature. It was found that a large majority of the models do not predict the ignition delay times with accuracy, and there is a surprisingly wide variation amongst the predictions. One satisfactory model, from Dagaut et al. (2008), was selected and extended to compounds other than NH₃ using H₂/O₂/CO, N₂O, NO₂, and NNH sub-mechanisms from the literature. The resulting comprehensive mechanism predicts well the ammonia ignition delay time data from the present study along with other NH₃, NO₂, and N₂O data from the authors as well as from the literature with high accuracy. In addition to the new ammonia oxidation data and related model comparisons, the present paper documents a state-of-the-art NOx sub-mechanism that can be used for a wide range of combustion calculations when added to, for example, baseline mechanisms involving hydrogen and hydrocarbon kinetics.

© 2014 The Combustion Institute. Published by Elsevier Inc. All rights reserved.

1. Introduction

Ammonia (NH₃) is an impurity commonly found in gaseous fuels derived from the gasification processes of biomass [1] or coal [2] and is one of the largest sources of nitrogen leading to NO formation during coal combustion [3]. Depending on the conditions under which coal or biomass volatile matter is burned, the ammonia can either be converted to NO (fuel-NOx (oxides of nitrogen) formation mechanism) or to N₂ [3–6]. Ammonia has also a key role in de-NOx processes [4,7–10] and can also be used directly as a fuel in internal combustion engines [11,12] or as a hydrogen vector [12]. Since NOx emissions from industrial processes and energy production plants have been a concern for decades, a large body of research on NH₃ oxidation – NOx formation/removal in flames [12–21], shock tubes [22–34,7,35,36] or flow reactors [3,37–42] – is now available. In parallel with this large body of experimental studies, a great number of detailed combustion mechanisms

containing ammonia sub-mechanisms are currently available in the literature [5,12,43–49].

Despite this extensive number of studies, more work is still required to further validate the model over a wider range of conditions (as shown by some recent studies focusing on fuel rich – intermediate temperature [42] or oxy-combustion conditions [50]) or to clarify certain reaction pathways (such as the study on the role of NNH in NO formation and control using NH₃ as a reducing agent by Klippenstein et al. [49]). For instance, it is worth mentioning that the pressure domain above 10 atm remains fairly unexplored with regard to NH₃. In fact, to the best of the authors' knowledge, only the shock-tube study of Drummond [33], where ignition delay times were measured, has been performed above 10 atm. However, this high-pressure set of data is provided for a broad yet unclear range of pressure, reported to be between 27.2 and 44.4 atm, which makes it difficult to use these data to validate a model. Shock-tube ignition delay time measurements under well-defined conditions for pressures in excess of 10 atm are therefore necessary to further validate NH₃ models at high pressure.

The modeling of ignition delay times (τ_{ign}) obtained in shock tubes is indeed a convenient way to assess the overall validity of

* Corresponding author.

E-mail address: olivier.mathieu@tamu.edu (O. Mathieu).

a detailed kinetics mechanism at high temperatures and well defined conditions. However, when modeling shock-tube data from the literature, large discrepancies in the results can be observed amongst the aforementioned detailed mechanisms, as can be seen from Fig. 1, where data from Fuji et al. [34] are compared to several literature models. Differences of more than an order of magnitude are observed between the mechanism from Dagaut et al. [47] and the mechanism of Mueller et al. [44].

Nonetheless, it is visible in this figure that the mechanisms from the literature do not predict correctly the experimental data, especially on the lower-temperature side, and there are large differences amongst the various mechanisms. Literature kinetics models can be separated into two groups: under- and over-reactive mechanisms. The best mechanism from the over-reactive group is the mechanism of Konnov and De Ruyck [41] with a factor around 2 between the experiments and the calculation. The other mechanisms from this group are either older [44] or are based on this mechanism [12,48]. It is interesting to note that the group of the under-reactive mechanisms is composed of the more-recent mechanisms (if we exempt the mechanism from Miller and Bowman [5]). These mechanisms present good to acceptable predictions at high temperatures, above 1800 K, but are not reactive enough, by a factor between two and three, below this temperature. However, a further analysis of the data shows that it would be difficult to fully assess the validity of these detailed kinetics models based on the data in Fig. 1 or with other ignition delay time data obtained in shock tubes from the literature. Unfortunately, most of the shock-tube studies from the literature do not report the pressure and/or temperature conditions with an acceptable level of precision. For example, the pressure in Fig. 1 was reported as 2.5–7.5 atm in Fuji et al. [34], so the modeling was therefore conducted at an intermediate pressure of 5 atm. This difference in pressure can partly explain the disagreement observed between the models and the data.

In addition, it is important to mention that ammonia adsorbs on stainless steel, a material typically used to build shock tubes. Hence, accurate measurements necessitate a passivation of the shock-tube surfaces before conducting the experiment [4,7]. Unfortunately, no shock-tube studies where ignition delay times are measured report such passivation of the reactor's walls. This lack of wall passivation means that mixtures from the literature could present concentrations in ammonia that are probably lower than what was actually reported in the papers, depending on the surface polishing and the material of the shock tube considered. This systematic uncertainty could lead to equivalence ratios that are smaller than those reported, particularly for diluted mixtures where the NH₃ concentration is low, which constitutes most of the data available in the literature. One can therefore conclude that new shock-tube ignition delay time measurements with well-characterized and high-pressure conditions, with surface passivation, would be necessary to further develop and validate NH₃ models.

The first objective of this study was therefore to measure ignition delay times for NH₃ mixtures highly diluted (98–99% Ar dilution) in a shock tube. Experiments were performed behind reflected shock waves, after surface passivation of the reactor walls, for pressures around 1.4, 11, and 30 atm and for equivalence ratios set to 0.5, 1.0, and 2.0. These data were then compared to the literature mechanisms. A detailed chemical kinetics model was then selected, and the second main objective of the present study was therefore to improve this mechanism to also predict correctly a wide range of NH₃, HCN, and H₂/NOx data from the literature. Details on the experimental procedure are covered first, followed by the experimental results and the model's improvement and validation stages.

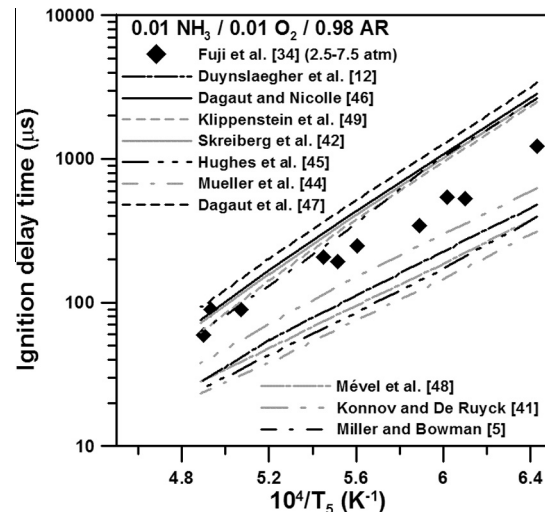


Fig. 1. Comparison between experimental data from Fuji et al. [34] and available models from the literature. Experimental data are given for a pressure range between 2.5 and 7.5 atm, and the modeling was performed at 5 atm.

2. Methods

The single-diaphragm, stainless steel, shock tube used during this study has a driven section that is 15.24-cm i.d., 4.72-m long, and a driver section that is 7.62-cm i.d., 2.46-m long. Details and schematics of the shock-tube setup can be found in Aul et al. [51]. Five PCB P113A piezoelectric pressure transducers, equally spaced alongside the driven section and mounted flush with the inner surface were used along with four Fluke PM-6666 timer/counter boxes to measure the incident-wave velocities. A curve fit of these four velocities was then used to determine the incident wave speed at the endwall location. Post reflected-shock conditions were obtained using this extrapolated wave speed in conjunction with one-dimensional shock relations and the initial conditions at the test region. This method was proven to maintain the uncertainty in the temperature determination behind reflected shock waves (T_5) below 10 K [52]. Test pressure was monitored by one PCB 134A transducer located at the endwall and one Kistler 603 B1 transducer located at the sidewall, in the same plane as the observation windows (Sapphire, located 16 mm from the endwall). Non-ideal boundary layer effects measured by the change in pressure (dP/dt) behind the reflected shock wave were determined to be less than 2% per ms for all experiments. The corresponding increase in temperature for these dP/dt levels would be less than 10 K for the longest ignition delay times reported in this study and therefore does not have a noticeable impact on the results herein.

Experiments were performed at three different pressure conditions (around 1.4, 11, and 30 atm), and three equivalence ratios (ϕ), 0.5, 1.0, and 2.0. Polycarbonate diaphragms were used for test pressures of 1.4 and 11 atm (0.25-mm and 2 × 1.02-mm thickness, respectively), while pre-scored aluminum diaphragms (2.29-mm thickness) were used for the 30-atm experiments. When polycarbonate diaphragms were used, a cross-shaped cutter was employed to facilitate breakage of the diaphragm and prevent diaphragm fragments from tearing off. Helium was used as the driver gas during this study.

The driven section was vacuumed down to 2×10^{-5} Torr or better using a roughing pump and a Varian 551 Turbomolecular pump prior to every run. The pumping time between experiments was minimized using a pneumatically driven poppet valve matching the inside diameter of the driven section and allowing for a passage

of 7.62-cm diameter between the vacuum section and the driven tube. The pressure was measured using two MKS Baratron model 626A capacitance manometers (0–10 Torr and 0–1000 Torr) and an ion gauge for high vacuums. Test mixtures were prepared manometrically in a mixing tank of 3.05-m length made from stainless steel tubing with a 15.24-cm ID. The pressure in the mixing tanks was measured using a Setra GCT-225 pressure transducer (0–17 atm). The mixing tank is connected to the vacuum system and can be pumped down to pressures below 1×10^{-6} Torr. The gases (Ammonia (Praxair, 99.9% purity diluted in 94.92% Ar (99.999% purity)), O₂ (Praxair, 99.999% purity), and Ar (Acetylene Oxygen Company, 99.999% purity)) were passed through a perforated stinger traversing the center of the mixing tank to allow for rapid, turbulent mixing. To further ensure homogeneity through diffusion processes, mixtures were allowed to rest for at least 1 h prior to making the first run. No difference in the results was observed for longer mixing times.

Since NH₃ adsorbs on stainless steel [4,53], the mixing tank and shock-tube surfaces were passivated with NH₃ before the mixture preparation and before each experiment. The passivation method was as follows: introduction of around 100 Torr of NH₃ for at least 5 min in the vessel (i.e. mixing tank or shock tube) and then vacuuming for 5 min with the rough pump (until around 40 mtorr, typically) before filling with the mixture (shock tube) or mixture components (mixing tank). Mixtures and conditions investigated during this study are summarized in Table 1.

The ignition delay time was measured using the chemiluminescence emission from the A²Σ+ → X²Π transition of the excited-state hydroxyl radical (OH*) using an interference filter centered at 307 ± 10 nm with a Hamamatsu 1P21 photomultiplier tube in a custom-made housing. The ignition delay time is defined herein as the time between the passage of the reflected shock wave, indicated by a pressure jump in the signal delivered by the sidewall pressure transducer, and the intersection of lines drawn along the steepest rate-of-change of OH* de-excitation and a horizontal line which defines the zero-concentration level, as can be seen in Fig. 2. Time zero is defined as the time of arrival of the reflected shock wave at the sidewall measurement location. Note the typical OH* profiles for NH₃ at this pressure condition, where the OH* signal does not come back to zero and stays flat for a few hundred microseconds (at least) after the ignition. All of the data signals were recorded through a 14-bit GageScope digital oscilloscope with sampling rates of 1 MHz or greater per channel.

There are essentially two sources of uncertainties in the ignition delay time: the uncertainty in the determination of the temperature behind the reflected shock wave (T_5) and the uncertainty associated with the determination of the steepest rate of change from the OH* profile. The temperature determination is

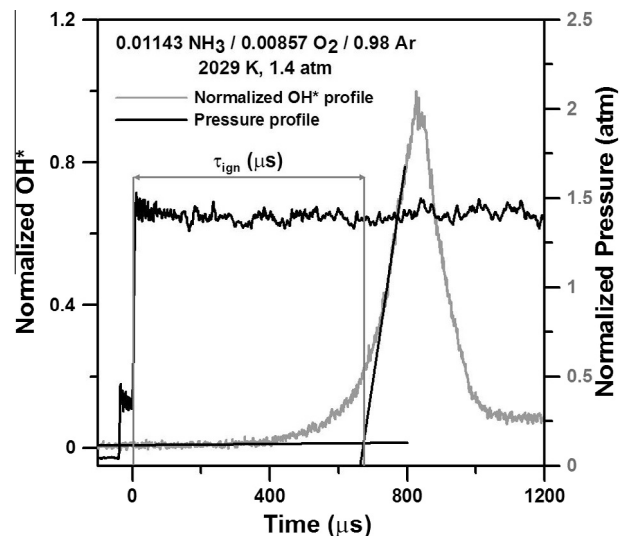


Fig. 2. Typical pressure and OH* profiles and method of determination of the ignition delay time.

the most important uncertainty and, as mentioned earlier, the experimental setup and method used allow for a determination of T_5 within less than 10 K. Thanks to the high signal/noise ratio of the experimental signals, the second source of uncertainty was small and can be neglected. Overall, the total uncertainty in τ_{ign} reported in this study is estimated to be 10% (which also includes the minimal temperature variation with facility dP/dt).

3. Experimental results

3.1. Equivalence ratio effect

The equivalence ratio effects on the ignition delay times for ammonia are visible in Fig. 3 at pressures around 1.4 atm (3a), 11 atm (3b), and 30 atm (3c). As can be seen, at pressures of 11 atm and above, the ignition delay times obtained at $\phi = 1.0$ and 2.0 are very similar, while ignition delay times obtained at $\phi = 0.5$ are shorter (by a factor around 1.5). At the lowest pressure investigated, around 1.4 atm (Fig. 3a), the equivalence ratio seems to have only a moderate effect on τ_{ign} . However, at this lower-pressure condition, ignition delay times at the stoichiometric condition seem to be longer than for the other conditions (although ignition delay times at $\phi = 0.5$ are similar for high temperatures). The activation energies (Ea) extracted from Fig. 3 show that Ea does not vary much with the equivalence ratio at 11 atm and above (Ea = 39.5, 40.1, and 40.1 kcal/mol at 11 atm for $\phi = 0.5$, 1.0, and 2.0, respectively and Ea = 42.5, 42.0, and 44.1 kcal/mol at 30 atm for $\phi = 0.5$, 1.0, and 2.0, respectively). However, it seems that Ea increases slightly with the equivalence ratio for the lowest pressure investigated: Ea = 44.6, 51.7, and 56.3 kcal/mol for $\phi = 0.5$, 1.0, and 2.0, respectively, at 1.4 atm. Note that this result could partly come from the small amount of curvature observed on the low-temperature side of the curve.

3.2. Pressure effect

As can be seen in Fig. 4(a–d), there is an important effect of pressure on the ignition delay time of the ammonia–oxygen–argon mixtures, for all the equivalence ratios and levels of Ar dilution investigated. It is visible in this figure that the ignition delay time decreases with the increase in the pressure. A factor around 7 is found between ignition delay times obtained at 1.4 and 11 atm at 2000 K for all conditions investigated, while smaller factors of

Table 1
Experimental conditions investigated behind reflected shock waves.

Mixture composition (mole fraction)	Equivalence ratio (ϕ)	T_5 (K)	P_5 (atm)
0.004 NH ₃ /0.006 O ₂ /0.99 Ar	0.5	1925–2480	1.4 ± 0.1
		1625–2015	10.9 ± 0.5
		1560–1895	28.7 ± 1.0
0.005715 NH ₃ /0.004285 O ₂ /0.99 Ar	1.0	1985–2490	1.4 ± 0.1
		1660–2080	10.8 ± 0.4
		1565–1930	28.7 ± 1.0
0.01143 NH ₃ /0.00857 O ₂ /0.98 Ar	1.0	1825–2455	1.4 ± 0.1
		1615–2085	10.5 ± 0.4
		1565–1870	28.6 ± 0.6
0.007273 NH ₃ /0.002727 O ₂ /0.99 Ar	2.0	1990–2360	1.4 ± 0.1
		1650–2040	10.6 ± 0.6
		1580–1910	28.9 ± 1.5

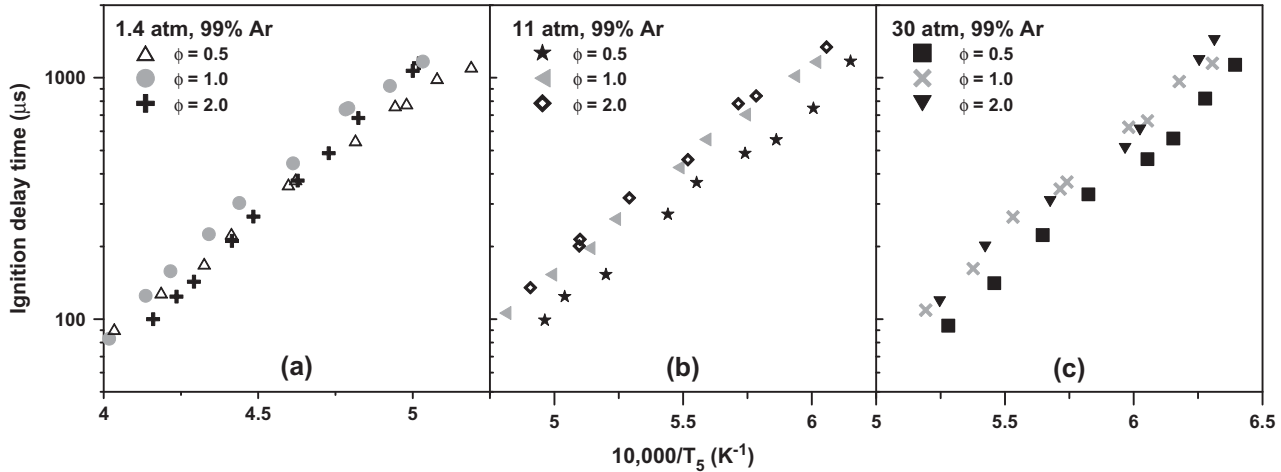


Fig. 3. Effects of the equivalence ratio on the ignition delay time of NH_3 mixtures diluted in 99% Ar at around (a) 1.4 atm, (b) 11 atm, and (c) 30 atm.

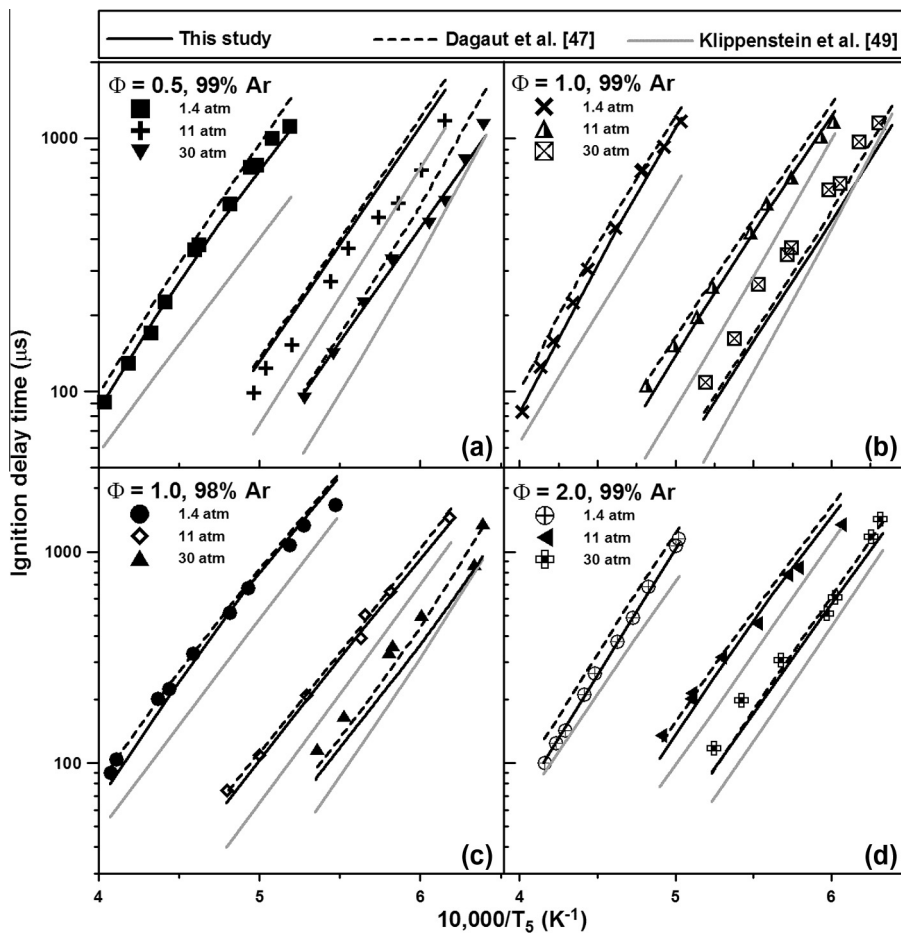


Fig. 4. Effects of the pressure on the ignition delay time of NH_3 mixtures at equivalence ratios of (a) 0.5, 1.0 ((b) 99% and (c) 98% Ar dilution) and (d) 2.0. Lines correspond to modeling. Black line: this study, dashed line: Dagaut et al. [47], grey line: Klippenstein et al. [49].

1.8, 1.9, and 2.2 were found at 1700 K amongst τ_{ign} obtained at 11 and 30 atm for $\phi = 0.5$, 1.0 (at both dilution levels), and 2.0, respectively.

3.3. Fuel concentration effect

By comparing the data obtained at $\phi = 1.0$ for the 98% and 99% dilution in Ar cases, Fig. 5, one can see the effect of a factor 2 of the

NH_3 concentration on the ignition delay time. As can be seen in this figure, at around 1.4 atm (5a), ignition delay times are typically shorter for the 98% dilution case. However, the ignition delay times tend to converge toward a similar value as the temperature increases, τ_{ign} being similar for temperatures above 2270 K. For higher pressures, 11 atm (Fig. 5b) and 30 atm (Fig. 5c), the ignition delay times are also shorter for the lowest dilution ratio, and also tend to converge toward a similar value at a given temperature.

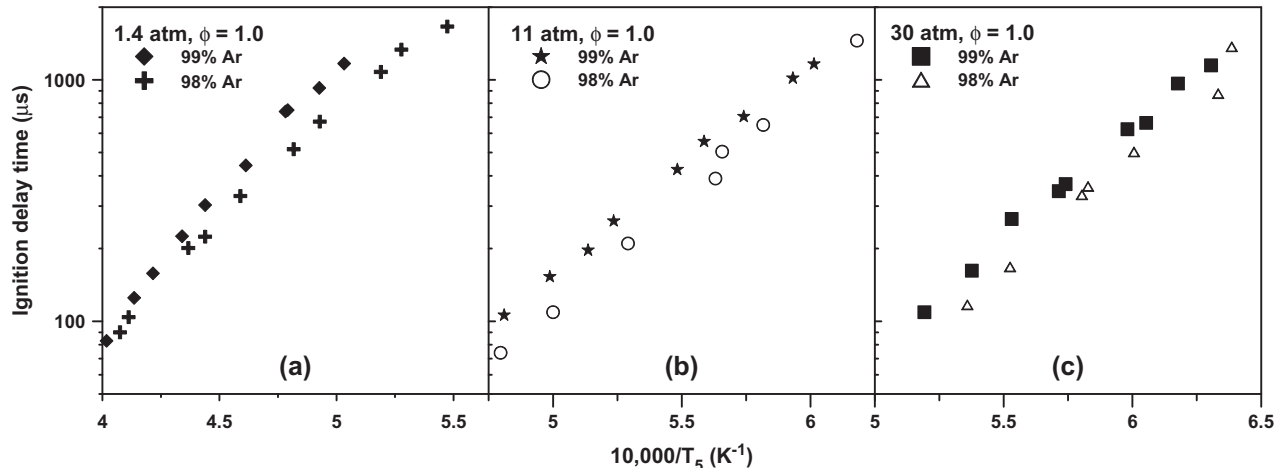


Fig. 5. Effect of the dilution level (98 and 99% Ar) on the ignition delay time of NH₃ at around (a) 1.4 atm, (b) 11 atm, and (c) 30 atm and at $\phi = 1.0$.

However, for these higher-pressure cases, ignition delay times converge toward the same value on the lower-temperature side. Activation energies for the mixtures with 98% Ar dilution are 42.0, 43.0, and 46.7 kcal/mol at 1.4, 11, and 30 atm, respectively. These values compare with the value obtained for the 99% Ar dilution, except for the low-pressure case where E_a is higher for the highest dilution level (51.7 kcal/mol).

Using the shock-tube data presented herein, it was possible to derive the following correlation ($r^2 = 0.955$), with P in atm and T_5 in K:

$$\tau_{\text{ign}}(\mu\text{s}) = 16.81 \cdot 10^{-3} \varphi^{0.18} P^{-0.89} \exp(44.11 \text{ (kcal)}) / RT_5 \quad (\text{R1})$$

The comparison between the ignition delay time values measured experimentally and determined with the correlation (R1) is visible in Fig. 6.

All of the ignition delay time measurements along with their corresponding conditions behind the reflected shock waves are provided in Table 2.

3.4. Comparison with models from the literature

To assess the validity of the aforementioned detailed kinetics models, data from this study were modeled with mechanisms available in the literature. To compare fairly with the experimental OH* profile, the OH* sub-mechanism from Hall and Petersen [54] was merged to these detailed kinetics mechanisms whenever necessary. Due to the large differences observed in some conditions between the computed and experimental ignition delay time and shapes of the OH* profile, it was found necessary to add the reaction N₂O + H \rightleftharpoons N₂ + OH* from Hidaka et al. [55] to the OH* scheme from Hall and Petersen. Figure 7 shows some representative normalized experimental OH* profiles that have been modeled using the mechanism from Dagaut et al. [47] along with the OH* chemistry from Hall and Petersen [54] and with and without the aforementioned OH* formation reaction from Hidaka et al. [55]. As can be seen, this combination of reactions allows for a good comparison between model and experiment for both the profiles and ignition delay times, whereas a strong disagreement in the shape (Fig. 7a and 7c) and in the ignition delay time can be observed without the OH* formation from the N₂O + H \rightleftharpoons N₂ + OH* reaction. Note that the normalized OH* profile does not reach 1 in Fig. 7c because the computed OH* profile increases and reaches its maximum value well after the time frame of Fig. 7c.

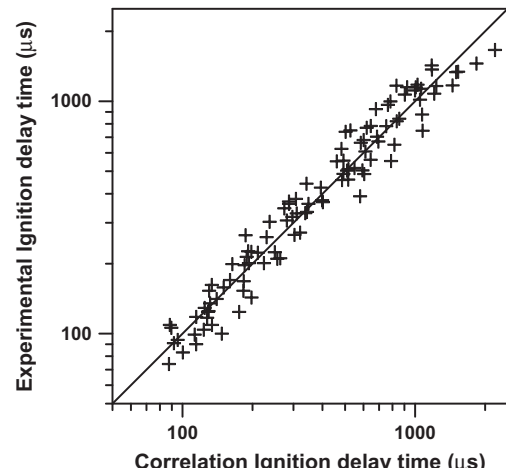


Fig. 6. Correlation compared to experiment values for ignition delay times measured during this study.

Using this complete OH* sub-mechanism, comparisons between some selected and representative data from this study and the models from the literature are visible in Fig. 8. As can be seen in Fig. 8, the mechanism of Dagaut et al. [47] predicts the experimental data with high accuracy regardless of the ammonia concentration, the pressure, or the equivalence ratio. At around 1.4 atm, however, the model tends to be slightly under-reactive but is still the closest to the experimental data. The model of Dagaut and Nicolle [46], although slightly too reactive, also provides acceptable results. As also seen in Fig. 8, the recent model of Klippenstein et al. [49] is close to the prediction of the model from Dagaut and Nicolle at stoichiometric conditions but is too reactive for the fuel-lean and fuel-rich conditions investigated. The model from Miller and Bowman [5] generally presents an activation energy that is too high and gives a mediocre prediction of τ_{ign} . The other mechanisms are somewhat close to each other in terms of predictions (within a factor 3) but are significantly too reactive, in addition to presenting too low of an activation energy. However, it is fair to mention that the mechanism of Duynslaeger et al. [12] was developed for low-pressure conditions only, hence explaining the poor agreement at high pressure, and that the model of Mével et al. [48] is essentially a model that aims primarily to predict the combustion of H₂/N₂O mixtures that also encompasses an ammonia sub-mechanism.

Table 2

Ignition delay times and associated conditions behind reflected shock waves.

0.004 NH ₃ /0.006 O ₂ /0.99 Ar			0.01143 NH ₃ /0.00857 O ₂ /0.98 Ar		
P ₅ (atm)	T ₅ (K)	τ _{ign} (μs)	P ₅ (atm)	T ₅ (K)	τ _{ign} (μs)
1.58	1927	1113	1.52	1827	1662
1.57	1969	998	1.43	1895	1334
1.53	2008	783	1.47	1927	1078
1.46	2023	769	1.42	2029	671
1.48	2077	551	1.41	2076	516
1.44	2164	380	1.38	2179	330
1.46	2175	362	1.33	2253	224
1.46	2266	226	1.25	2290	201
1.43	2312	170	1.28	2454	90
1.34	2389	129			
1.29	2479	91	10.9	1618	1453
			10.9	1719	650
11.4	1626	1170	10.5	1768	504
11.1	1665	747	10.1	1776	390
11.0	1706	553	10.8	1890	210
11.0	1742	486	10.8	2000	109
10.9	1801	368	10.5	2085	74
10.6	1838	272			
10.9	1923	153	29.7	1566	1370
10.9	1984	124	29.1	1579	877
10.4	2015	99	29.7	1665	503
			29.2	1716	362
29.7	1564	1132	28.0	1723	334
29.2	1593	820	28.2	1810	168
28.7	1625	560	28	1866	117
28.6	1652	460	0.007273 NH ₃ /0.002727 O ₂ /0.99 Ar		
0.005715 NH ₃ /0.004285 O ₂ /0.99 Ar			P ₅ (atm)	T ₅ (K)	τ _{ign} (μs)
P ₅ (atm)	T ₅ (K)	τ _{ign} (μs)			
1.51	1987	1167	1.49	1992	1149
1.45	2030	925	1.46	2000	1068
1.38	2087	749	1.49	2073	681
1.42	2091	739	1.46	2000	487
1.44	2168	442	1.44	2161	375
1.41	2253	303	1.37	2230	266
1.35	2304	225	1.35	2265	211
1.34	2372	158	1.37	2330	143
1.30	2418	125	1.37	2361	124
1.29	2489	83	1.37	2404	100
			11.3	1651	1340
11.2	1663	1163	11.0	1729	841
10.9	1686	1016	10.7	1750	781
11.0	1742	704	10.7	1812	458
10.8	1790	555	10.5	1890	318
10.8	1824	425	10.9	1961	214
10.6	1910	260	10.5	1962	201
10.6	1947	197	10.1	2038	135
10.8	2005	153	28.6	1584	1426
10.6	2079	106	28.9	1599	1179
			29.1	1660	608
29.1	1586	1148	30.4	1676	510
28.8	1619	965	29.2	1762	307
28.6	1652	663	28.5	1844	199
29.6	1672	624	27.5	1906	118
29.2	1742	370			
28.8	1750	346			
28.0	1808	265			
27.7	1860	162			
27.9	1926	109			

4. Improvement and validation of a NH₃/NOx mechanism

It can be deduced from Fig. 8 that the model from Dagaut et al. [47] is a convenient one for modeling ignition delay times with NH₃ over a wide range of conditions. This mechanism was therefore selected as a base to develop a more-comprehensive

NH₃/NOx/H₂ model. As mentioned earlier, NH₃ can play a great role in the production and control of NOx species in industrial applications. A great example of the NOx/NH₃ interactions was provided earlier with the OH* profile predictions, where the N₂O chemistry was seen to be of great importance for the NH₃ combustion, the reaction N₂O + H ⇌ N₂ + OH* being critical for the determination

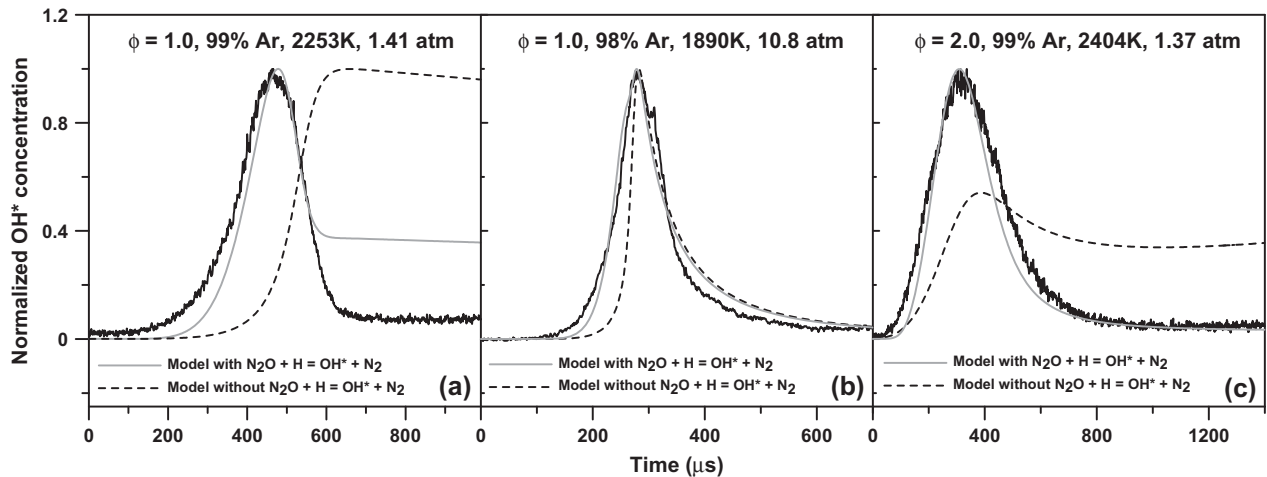


Fig. 7. Comparison of the temporal evolution of the experimental and computed OH^* profiles. Model: Dagaut et al. [47] along with the OH^* chemistry from Hall and Petersen [54] with and without the additional OH^* formation reaction from Hidaka et al. [55], for various conditions representative of those investigated during this study.

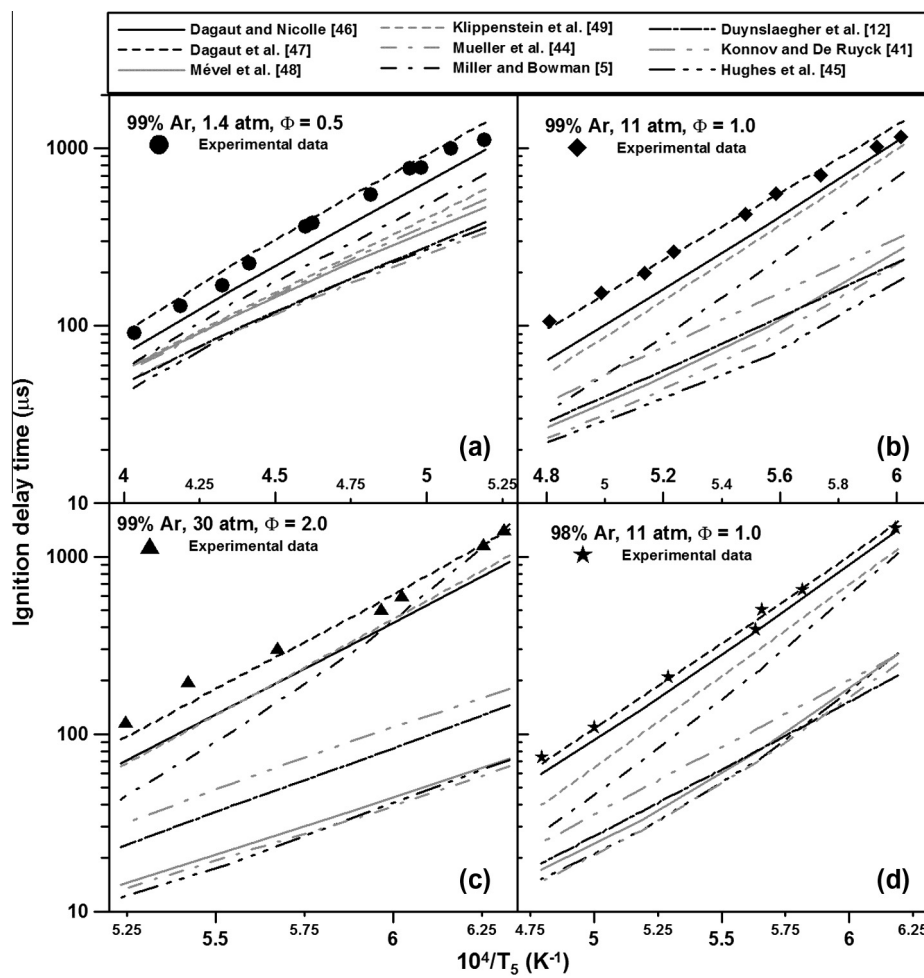


Fig. 8. Comparison between models from the literature and selected, representative data from this study. (a): 1.4 atm, $\phi = 0.5$, 99% Ar, (b): 11.0 atm, $\phi = 1.0$, 99% Ar, (c): 30 atm, $\phi = 2.0$, 99% Ar and (d): 11.0 atm, $\phi = 1.0$, 98% Ar.

of τ_{ign} with NH_3 data using the OH^* diagnostic. One of the objectives of this study was therefore to assess the validity of the model from Dagaut et al. [47] over NH_3 and NO_x data from the literature and to improve the mechanism without deteriorating the good

predictions on the shock-tube data from the present study. The predictions from this improved mechanism and the model from Dagaut et al. [47] were also compared to the predictions of the most recent NH_3 model from the literature (Klippenstein et al.

Table 3

Literature data selected as a target to validate the model.

Target	Type of data	Conditions	Reference
NH ₃	τ_{ign} in shock tube (OH* onset) NH, NH ₂ profiles and peak value in shock tube	See Table 1 Pyrolysis, 2200–2800 K, around 1 atm	This study Davidson et al. [36]
NH ₃ /N ₂ O	τ_{ign} in shock tube (OH onset)	0.04 NH ₃ /0.06 N ₂ O/0.9 Ar, 1535–1825 K, 3.3–4.4 atm	Drummond [56]
N ₂ O	τ_{ign} in shock tube (OH* onset)	0.01 H ₂ /0.01 O ₂ /0.98 Ar + 0, 100, 400, 1600, and 3200 ppm of N ₂ O, 1.7–32 atm	Mathieu et al. [57]
	τ_{ign} in shock tube (time at 50% of maximum OH* signal)	H ₂ /N ₂ O mixtures, 1300–2000 K, 0.5 < ϕ < 2.0, 98–99% Ar, 3–9 atm	Mével et al. [48]
	Time at 50% and 80% of N ₂ O consumption	N ₂ O/H ₂ /Ar mixtures, 1400–2000 K, 3 atm	Hidaka et al. [58]
	Time at the peak of OH* profile	0.005 H ₂ /0.01 N ₂ O/0.03 CO/0.9595 Ar, 1654–2221 K, 1.4 and 10 atm	Kopp et al. [59]
NO ₂	τ_{ign} in shock tube (OH* onset)	0.01 H ₂ /0.01 O ₂ /0.98 Ar + 0, 100, 400, and 1600 ppm of NO ₂ , 1.7–33 atm	Mathieu et al. [60]
	H ₂ oxidation with NO or NO ₂ addition in a jet stirred reactor	1 & 10 atm, 0–50 ppm NO ₂ , 0–200 ppm NO, 10,000 ppm H ₂ in N ₂	Dayma and Dagaut [61]
HCN	τ_{ign} in shock tube (time at 10% peak OH) N, O, H absorption traces	1% HCN/1% O ₂ in Ar, 1885–2630 K, 1 atm 50–100 ppm HCN/50–1000 ppm O ₂ in Ar, 2600–2836 K, 1.69–1.82 atm	Higashihara et al. [62] Thielen and Roth [63]

Table 4

List of the sub-mechanisms used to assemble the mechanism proposed in the present study.

Sub-mechanism	Reference
H ₂ /CO	Kéromnès et al. [64]
NH ₃	Dagaut et al. [47]
HCN	Dagaut et al. [47]
N ₂ O	Mathieu et al. [57]
NO ₂	Dayma and Dagaut [61] with high-pressure updates from Sivaramakrishnan et al. [67]
NNH	Klippenstein et al. [49]

[49]). Data selected for the model improvement and validation are summarized in Table 3.

The first improvement to the mechanism from Dagaut et al. [47] was to update the H₂/O₂ chemistry with the recent H₂/CO/O₂ model from Kéromnès et al. [64]. This replacement of H₂/O₂ chemistry has nearly no effect on the predictions for the ignition delay times with NH₃ from the present study but improves the predictions against some literature data involving mixtures with H₂ and O₂. The second stage of the mechanism development consisted of improving the N₂O predictions, to validate the model on the particular link between NH₃ and N₂O previously observed with OH* profiles. Reactions involving N₂O have then been replaced by the ones selected in the H₂/N₂O mechanism proposed recently by the authors in Mathieu et al. [57]. The reactions involving NO₂ in the model proposed herein have been selected based on the work done in Mathieu et al. [60] where it has been seen that the NO₂ chemistry from Dayma and Dagaut [61] with the high-pressure updates from Sivaramakrishnan et al. [67] and with the reaction rate coefficient for the reaction H₂ + NO₂ ⇌ HONO + H from Parks et al. [68] accurately modeling these results. Table 4 presents the sub-mechanisms used to assemble the mechanism proposed in the present study. To provide further details on the model proposed in this paper, the reactions that have been modified in the model from Dagaut et al. [47] are listed in Table 5 (apart from the H₂/CO chemistry integrally coming from Kéromnès et al. [64]).

4.1. N₂O sub-mechanism validation

Figures 9–13 show comparisons between the N₂O data selected (Table 3) and the models selected (Table 4). Hidaka et al. [58] followed the temporal evolution of the N₂O concentration for a

Table 5List of reactions that have been modified in or added to the mechanism from Dagaut et al. [47] (in addition to the change in the H₂/CO chemistry from Kéromnès et al. [64]).

Reaction	Reaction rate (cm, mol, s, cal)			Source
	A	n	E	
N ₂ O + M ⇌ N ₂ + O + M	9.9 × 10 ¹⁰	0	57,960	[65]
Low pressure limit	6.62 × 10 ¹⁴	0	57,500	
N ₂ O + H ⇌ N ₂ + OH	3.31 × 10 ¹⁰	0	5090	[65]
Duplicate	7.83 × 10 ¹⁴	0	19,390	
N ₂ O + OH ⇌ N ₂ + HO ₂	2 × 10 ¹²	0	40,000	[48]
NO ₃ ⇌ NO + O ₂	2.5 × 10 ⁶	0	12,120	[66]
NO ₃ + NO ₃ ⇌ NO ₂ + NO ₂ + O ₂	5.12 × 10 ¹¹	0	4870	[66]
N ₂ O ₄ (+M) ⇌ NO ₂ + NO ₂ (+M)	4.05 × 10 ¹⁸	-1.1	12,840	[66]
Low pressure limit	1.96 × 28	-3.8	12,840	
N ₂ O ₄ + O ⇌ N ₂ O ₃ + O ₂	1.21 × 10 ¹²	0	0	[66]
N ₂ O ₃ + O ⇌ NO ₂ + NO ₂	2.7 × 10 ¹¹	0	0	[66]
N ₂ + M ⇌ N + N + M	1.89 × 10 ¹⁸	-0.85	224,950	[67]
N + O + M ⇌ NO + M	7.6 × 10 ¹⁴	-0.1	-1770	[67]
N ₂ + O ⇌ N + NO	1 × 10 ¹⁴	0	75,490	[67]
NO + OH(+M) ⇌ HONO(+M)	1.99 × 10 ¹²	-0.05	-721	[67]
NO + H + M ⇌ HNO + M	3 × 10 ²⁰	-1.75	0	[67]
NO ₂ + H ₂ ⇌ HONO + H	1.3 × 10 ⁴	2.76	29,770	[68]
NO ₂ + M ⇌ NO + O + M	1.1 × 10 ¹⁶	0	66,000	[67]
NO ₂ + NO ₂ ⇌ NO + NO + O ₂	2 × 10 ¹²	0	26,825	[67]
NO ₂ + HO ₂ ⇌ HONO + O ₂	1.91	3.32	3044	[67]
NO ₂ + NO ⇌ N ₂ O + O ₂	1 × 10 ¹²	0	60,000	[67]
HONO + OH ⇌ NO ₂ + H ₂ O	1.3 × 10 ¹⁰	1	135	[67]
HNO + O ⇌ NO + OH	1 × 10 ¹³	0	0	[67]
HNO + NO ₂ ⇌ NO + HONO	4.42 × 10 ⁴	2.6	4060	[67]
HNO + HNO ⇌ N ₂ O + H ₂ O	3.95 × 10 ¹²	0	5000	[67]
HNO + NO ⇌ N ₂ O + OH	2 × 10 ¹²	0	26,000	[67]
N + NO ₂ ⇌ N ₂ O + O	1.8 × 10 ¹²	0	0	[67]
N + O ₂ ⇌ NO + O	6.4 × 10 ⁹	1	6280	[67]
N + OH ⇌ NO + H	3.8 × 10 ¹³	0	0	[67]
N ₂ O + N ⇌ N ₂ + NO	1 × 10 ¹³	0	19,870	[67]
H ₂ NO + M ⇌ H ₂ + NO + M	3.83 × 10 ²⁷	-4.29	60,300	[67]
HO ₂ + NO + M ⇌ HONO ₂ + M	2.23 × 10 ¹²	-3.5	2200	[67]
HNO ₂ + H ⇌ NO ₂ + H ₂	2.4 × 10 ⁸	1.5	5087	[67]
HNO ₂ + O ⇌ NO ₂ + OH	1.7 × 10 ⁸	1.5	3020	[67]
HNO ₂ + OH ⇌ NO ₂ + H ₂ O	1.2 × 10 ⁶	2	-596	[67]
HNO ₂ ⇌ HONO	1.3 × 10 ²⁹	-5.47	52,814	[67]
HONO + NH ₂ ⇌ NO ₂ + NH ₃	71.1	3.02	-4941	[67]
HNO + N ⇌ NO + NH	1 × 10 ¹³	0	1990	[67]
NH + H ⇌ N + H ₂	1 × 10 ¹⁴	0	0	[5]
NNH + O ⇌ NH + NO	5.2 × 10 ¹¹	0.388	-409	[49]
NNH + O ⇌ N ₂ + OH	1.2 × 10 ¹³	0.145	-217	[49]
NH + NO ⇌ N ₂ O + H	1.8 × 10 ¹⁴	-0.351	-244	[49]
NH ₂ + NO ⇌ NNH + OH	3.1 × 10 ¹³	-0.48	1180	[49]

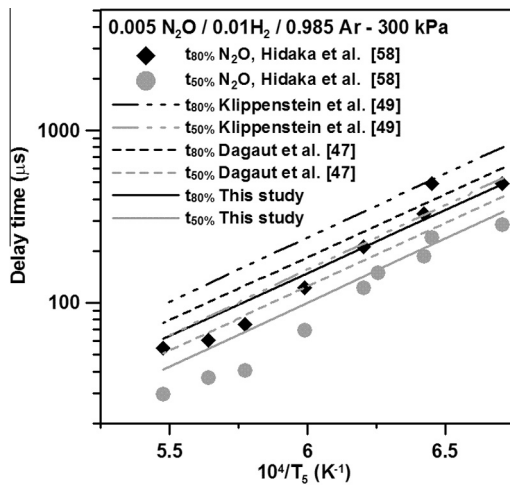


Fig. 9. Comparison between experimental data of Hidaka et al. [58] and the various model predictions for the time at which 50 and 80% of the N₂O is consumed at various temperatures for a 0.005 N₂O/0.01 H₂/0.985 Ar mixture at 300 kPa.

N₂O/H₂ mixture diluted in Ar. They determined the times at which the concentration of N₂O was 80 and 50% of the initial concentration (t_{80} and t_{50} , respectively) for several temperatures. As can be seen in Fig. 9, the model from the present study predicts t_{80} with accuracy over the entire range of temperature, while t_{50} is correctly reproduced overall, especially for the lowest temperatures. The models of Dagaut et al. and Klippenstein et al. are however predicting t_{50} and t_{80} that are too long. Compared to the t_{80} and t_{50} from the model proposed in this study, predictions from the model from Dagaut et al. [47] are around 25% longer, and this difference reaches 50–60% with the model from Klippenstein et al. [49].

The comparison between the models and the ignition delay time measurements from N₂/N₂O mixtures diluted in Ar from Mével et al. [48] are visible in Fig. 10. Results are the mostly the same for the two dilution levels at around 3 atm (Figs. 10a and 10b) or at high pressure (Fig. 10c): the models are close to each other and in good agreement, overall, with the data. The model from the present study presents the shortest ignition delay time predictions, which makes predictions in better agreement with the data on the low-temperature side. However, the agreement

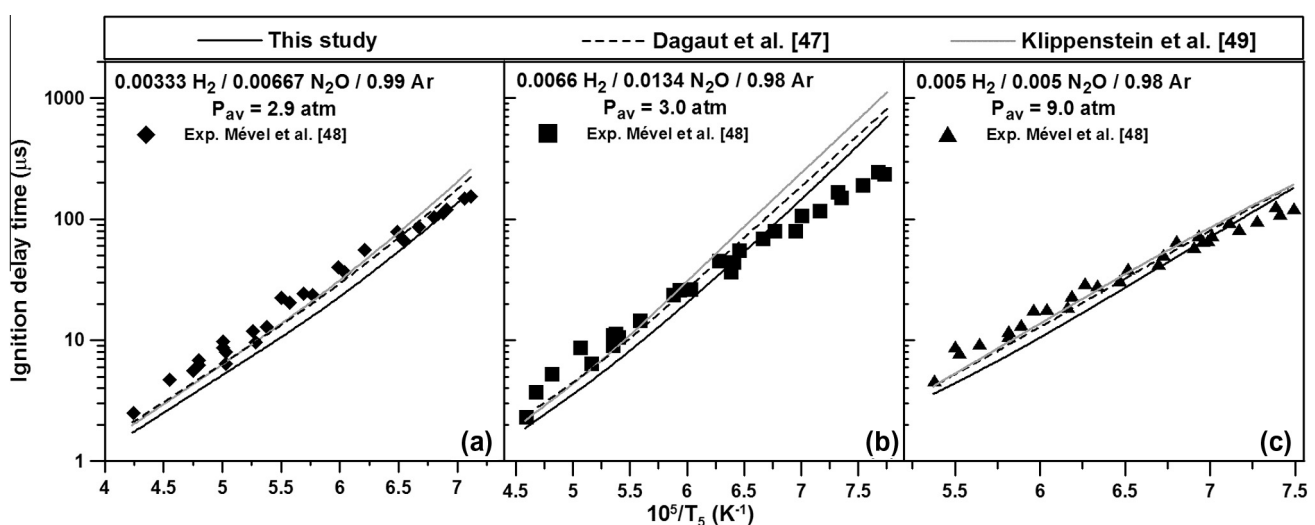


Fig. 10. Comparison between the experimental data of Mével et al. [48] and the model predictions.

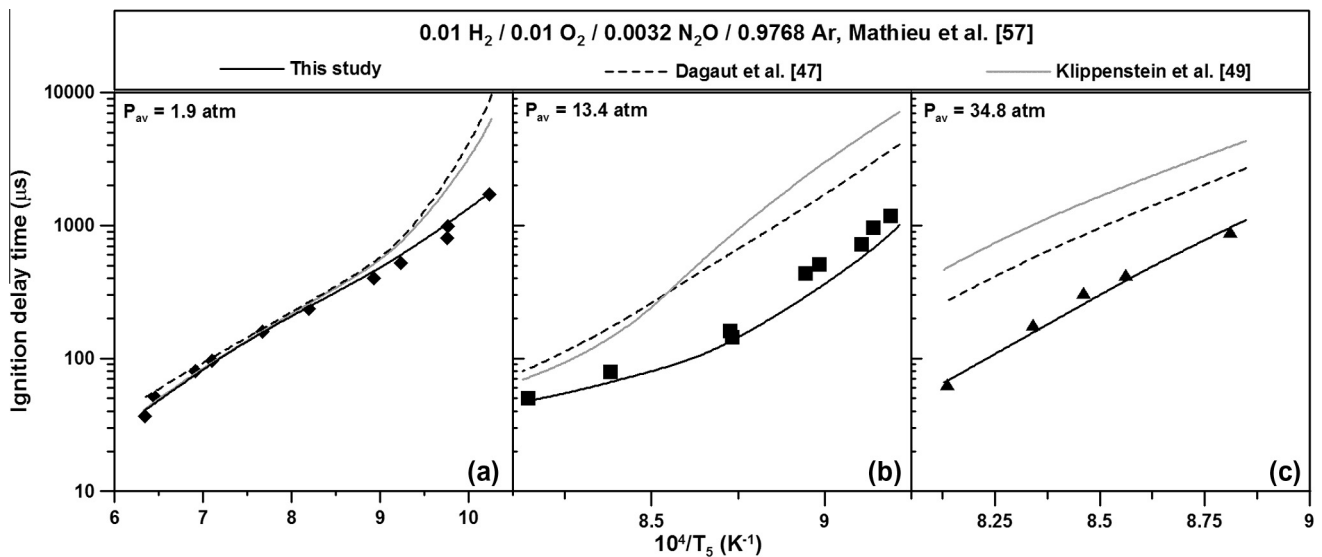


Fig. 11. Comparison between models and experiments from Mathieu et al. [57] for the ignition delay times of a 0.01 H₂/0.01 O₂/0.0032 N₂O mixture diluted in Ar at (a) around 1.9 atm, (b) around 13.4 atm, and (c) around 34.8 atm.

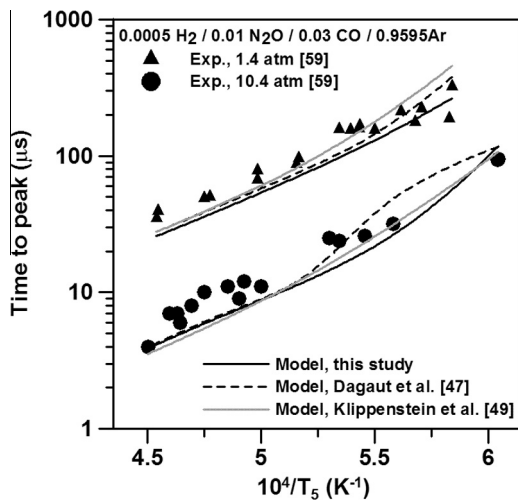


Fig. 12. Comparison between experimental data of Kopp et al. [59] and the various model predictions for the time at which the peak of the OH* profile was observed for a mixture of 0.0005 H₂/0.01 N₂O/0.03 CO/0.9595 Ar at around 1.4 and 10.4 atm.

with the data is not as good as with the other models at high temperature, although the difference with the experimental data is always on the order of a few tenths of a microsecond for the highest temperatures, which should largely be well within the experimental error factor.

The comparison between the models and the data from Mathieu et al. [57] with a H₂/O₂ mixture seeded with N₂O is visible in Fig. 11. As can be seen from this figure, the model from the present study predicts with high accuracy the ignition delay times over the entire range of temperature for the 3 pressure conditions investigated. At around 1.9 atm (Fig. 11a), one can see that the other models from the literature deviate rapidly from the experiments below 1100 K, where a difference by a factor of up to 5 is observed around 1000 K. For the intermediate pressure investigated (Fig. 11b), the literature models are in acceptable agreement with the data above 1200 K but significantly over-predict the ignition delay time below this temperature, by a factor 3 or more. A factor of 3 (Dagaut et al. [47]) to 4–5 (Klippenstein et al. [49]) was observed between the model and the data at the highest pressure investigated (Fig. 11c).

For the time-to-peak delays determined by Kopp et al. [59], it is visible in Fig. 12 that the model of the present study predicts the shortest delays at around 1.4 atm, the three models being very close in terms of predictions above 1900 K. Below this temperature, the peak times predicted by the models from the literature are increasing more rapidly than observed experimentally, which is not the case for the model of the present study. The general trend of the data at 10.4 atm is also well captured by the present model as well as by the model from Klippenstein et al. [49]. The model of Dagaut et al. [47], however, does not reproduce the experimental trend below 1900 K at this higher-pressure condition.

Note that the data from Mével et al. [48], Mathieu et al. [57], and Kopp et al. [59] have all been determined from OH* signals but at different locations of the signal: at the onset of the signal in Mathieu et al. [57], at 50% of the maximum intensity of the signal in Mével et al. [48] and at the time to peak for Kopp et al. [59]. The fact the model from the present study provides good predictions for all three of these datasets indicates that the key features of the OH* profiles (which depend on the accuracy of the fundamental stage chemistry) are well captured by the model, for different mixtures and over large ranges of pressure and temperature. Details on the choices for the reactions selected for the N₂O sub-mechanism can be found in Mathieu et al. [57].

4.2. NO/NO₂ sub-mechanism validation

The next stage of the mechanism development consisted of verifying the validity of the NO/NO₂ sub-mechanism. However, the amount of data involving NO/NO₂ that can be used to validate the combined mechanism herein is significantly smaller than for N₂O. Most of the literature data are focused on interactions between NO or NO₂ with hydrocarbons, which is beyond the scope of this study. To validate this sub-mechanism, the ignition delay times measured in a shock tube with H₂/O₂/NO₂ mixtures in Ar by Mathieu et al. [60] was used. As can be seen in Fig. 13, the data from Mathieu et al. [60] are well predicted by the various models, except for the data at 33 atm (Fig. 13c) for which the model of Dagaut et al. [47] is too reactive, especially on the lower-temperature side. At this high-pressure condition, the two other models yield nearly identical results. For the intermediate pressure, Fig. 13b, the model of the present study exhibits very accurate predictions (within the size of the data symbols) over the entire range

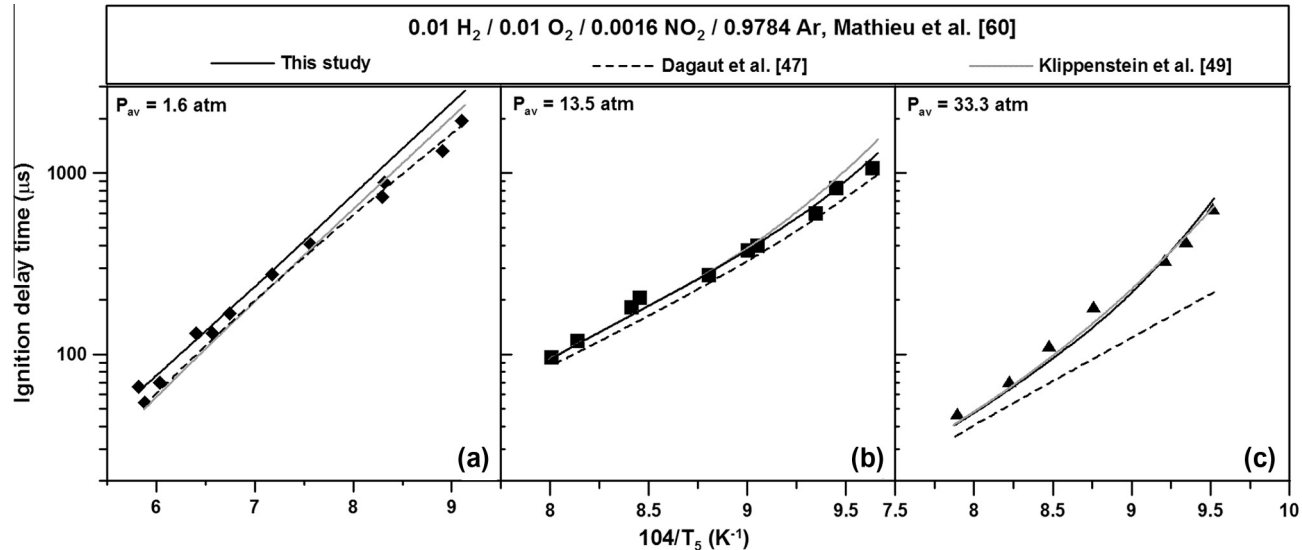


Fig. 13. Comparison between models and experiments from Mathieu et al. [60] for the ignition delay times of a 0.01 H₂/0.01 O₂/0.0016 NO₂ mixture diluted in Ar at (a) around 1.6 atm, (b) around 13.5 atm, and (c) around 33.3 atm.

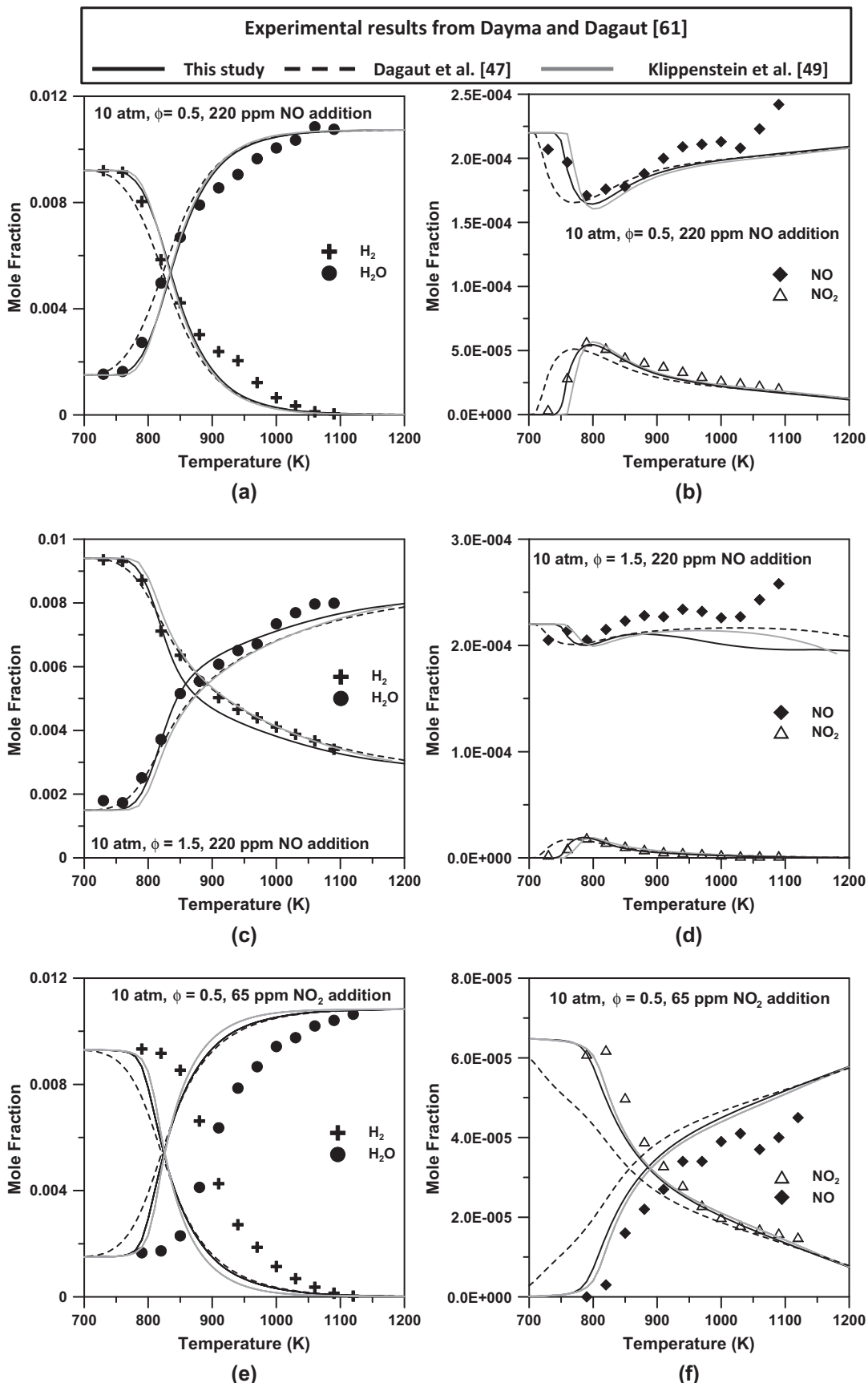


Fig. 14. Comparison between models and jet stirred reactor experiments from Dayma and Dagaut [61] of H_2/O_2 mixtures with NO or NO_2 addition.

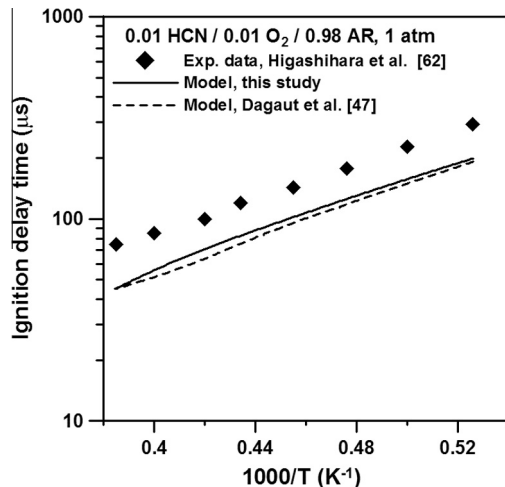


Fig. 15. Comparison between the models and the experiments from Higashihara et al. [62] for the ignition delay times of a 0.01 HCN/0.01 O₂ mixture diluted in Ar. The ignition delay times were determined at 10% of the peak value of the OH profile.

of temperature; whereas the model of Dagaut et al. is slightly over-reactive, and the model from Klippenstein et al. presents ignition delay times that are slightly too long on the lower-temperature side. For the lowest pressure condition investigated, Fig. 13a, the model from Dagaut et al. presents the best overall agreement with the data, especially on the lower-temperature side where the model of the present study is slightly under-reactive, but the present model is nonetheless also within the scatter of data over most of the temperature range.

Jet-stirred reactor data for H₂/O₂ mixtures seeded with either NO or NO₂ at various equivalence ratios from Dayma and Dagaut [61] have also been used to validate the model. These data have been modeled using the SENKIN module [69] of the PSR computer code [70]. Comparisons between the models and the data for some representative mixtures and conditions are presented in Fig. 14. Evolutions with the temperature for H₂ and H₂O, and NO and NO₂ at fuel lean conditions ($\phi = 0.5$) and in the presence of 220 ppm of NO are visible in Fig. 14a and Fig. 14b, respectively. At these conditions, the model of Dagaut et al. [47] is slightly over-reactive as the H₂ consumption (and the corresponding H₂O formation) starts at a temperature slightly lower than observed experimentally. The experimental profiles for these two species

are better reproduced by the model proposed in this study and by the model of Klippenstein et al. [49], especially for temperatures below 875 K. The over-reactivity of the model from Dagaut et al. is also visible on the NO/NO₂ profiles (Fig. 14b), where the conversion of NO to NO₂ starts about 40 K lower than the experiments. The NO and NO₂ profiles are well predicted by the model presented in this study, both in terms of temperature dependence and in the amplitudes of the humps. The model of Klippenstein et al. also presents good predictions, although the conversion of NO to NO₂ starts at slightly too-high of a temperature, and the amount of NO consumed at the peak is a little too high as well.

For the same mixture but at a fuel-rich condition ($\phi = 1.5$), the H₂ and H₂O profiles (Fig. 14c) are overall well predicted by the three models considered. The model from the present study captures the H₂O profile and low-temperature side of the H₂ profile the best, but the other models considered are closer to the H₂ data for temperatures above 825 K. As for the previous case, the first peaks of NO consumption/NO₂ formation, around 800 K, is better captured by the model of the present study (Fig. 14d). However, at temperatures higher than 900 K, the two other models are closer to the experimental data for the NO profile; although the second hump observed around 1025 K is captured by the model of the present study only. When NO₂ was added to the mixture, all models are noticeably over-reactive when compared to the experimental H₂ and H₂O profiles (Fig. 14e). As seen, the H₂ consumption/H₂O formation starts between 100 K (Dagaut et al.) and 50 K (model presented in this study and model from Klippenstein et al.) before the experimental profile. Note that the model from Klippenstein et al. is even more reactive than the two other models above 850 K. Concerning the NO and NO₂ profiles (Fig. 14f), the model from Dagaut et al. is still significantly over-reactive for these species, whereas the model presented in this study and the model from Klippenstein et al. are within an acceptable level of agreement with the data, the latest one being slightly closer to the experimental data.

4.3. HCN sub-mechanism validation

As mentioned by Dagaut et al. [47], HCN and NH₃ are intermediately formed during the combustion of coal and biomass fuels which contain N-bounded structures, and most of the HCN released subsequently forms NOx. It was therefore important to verify that the HCN chemistry developed in Dagaut et al. [47] was not altered by the changes made to the larger model in this

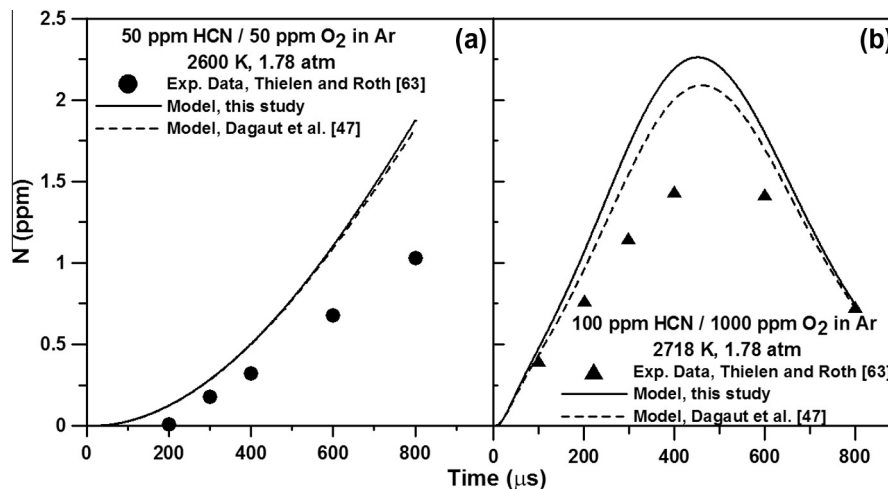


Fig. 16. Comparison between the models and the experiments for N mole fraction traces behind reflected shock waves for HCN/O₂ mixtures highly diluted in Ar at (a) 2600 and (b) 2718 K by Thielen and Roth [63].

study. The ignition delay times of a 0.01 HCN/0.01 O₂ mixture diluted in Ar was determined at 10% of the peak value of the OH profile by Higashihara et al. [62]. The comparison between these data and the model of Dagaut et al. and the modified model proposed in this study (note that the mechanism of Klippenstein et al. does not contain HCN and related species) is visible in Fig. 15. As can be seen in this figure, the original mechanism of Dagaut et al. is significantly over-reactive, a factor around 1.5 being observed compared to the experimental data. The modified model from this study predicts ignition delay times that are slightly longer and in a better agreement with the data, although the difference between the two models is slim, and both are similarly over-reactive.

Thielen and Roth [63] followed N, O, and H temporal profiles using highly diluted mixtures of HCN and O₂ in a shock tube. As can be seen in Fig. 16, the beginning of the rise in the N profile is well captured by the models, the two models almost yielding the same results, but the maximum value of the N profile is over-estimated. The model modified in the present study predicts levels of the N radical that are higher than the original mechanism from Dagaut et al. [47], although both versions similarly over-predict the peak N-atom mole fraction. Note that the decrease of the N radical after 600 μs for the high-temperature case (Fig. 16b) is well predicted by the two models.

The radical O profile from Thielen and Roth [66] is visible in Fig. 17. As can be seen, the agreement between both models and the data is good during the first 500 μs. For longer test times, the models tend to under-predict the quantity of O present in the reactive mixture. The model proposed in the present study deviates slightly from the original model after 400 μs and predicts a maximum amount of O radical that is about 0.5 ppm lower than the model of Dagaut et al. [47].

Figure 18 shows the comparison between the experiments from Thielen and Roth [63] and the models for the H radical. As can be seen, the experimental trend is well captured by the models, but the H concentration is significantly over-predicted by both after 400 μs. As for the N profiles, the model proposed in the present study predicts higher concentrations than the original model from Dagaut et al. [47].

4.4. NH₃ sub-mechanism validation

Predictions against NH₃ data from this study for the model proposed herein and for the two other reference models are visible in

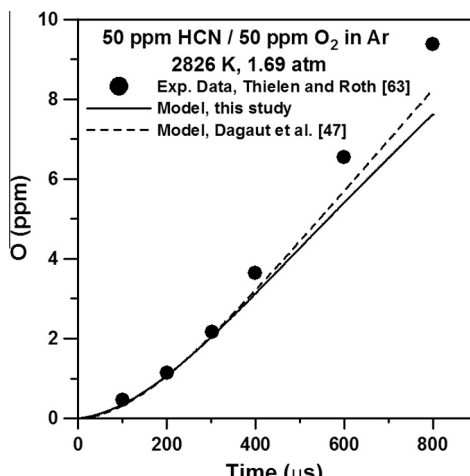


Fig. 17. Comparison between the models and the experiment for an O absorption trace behind reflected shock waves for a 50-ppm HCN/50-ppm O₂ mixture in Ar at 2826 K and 1.69 atm by Thielen and Roth [63].

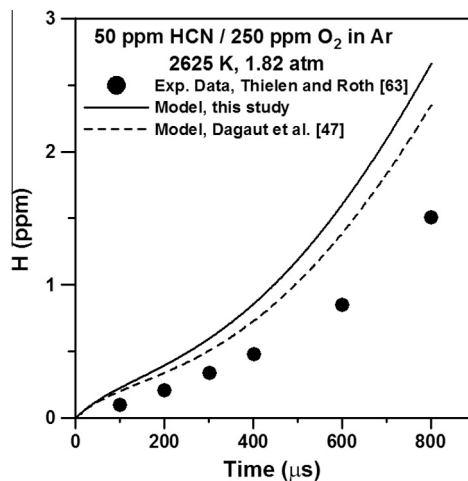


Fig. 18. Comparison between the models and the experiment for H-atom mole fraction behind reflected shock waves for a 50-ppm HCN/250-ppm O₂ mixture diluted in Ar at 2625 K and 1.82 atm by Thielen and Roth [63].

Fig. 4. As can be seen in this figure, the model from Klippenstein et al. [49] is consistently over-reactive. The disagreement with the data can reach a factor 2 to 3, although a smaller difference is generally observed. The ignition delay times at higher pressure (around 30 atm) are however well predicted at low temperatures for the stoichiometric and fuel-lean conditions. The models from Dagaut et al. [47] and from the present study (which is based on the model of Dagaut et al. [47]) are very close to each other and provide good predictions over the entire range of conditions investigated. The model proposed in this study is slightly more reactive than the model of Dagaut et al., which modestly improves the predictions in some cases ($\phi = 0.5$ at all pressure conditions, low-pressure data for the other equivalence ratios) but also slightly deteriorates them for certain cases (30-atm data at $\phi = 1$, for example). However, the two models can be viewed as good models to predict these kind of ammonia oxidation data.

The NH and NH₂ profiles from Davidson et al. [36] are useful for validating the pyrolysis chemistry of a NH₃ model since these authors passivated the wall of their shock tube prior to conducting their experiments. Figure 19 shows temporal NH profiles (19a) and maximum NH level for several NH₃ concentrations at various temperatures. As can be seen from Fig. 19a, the predictions of model from Dagaut et al. [47] have been significantly improved by the modifications made in the present study. The amount of NH predicted is much lower and closer to the experimental data for the two temperatures. This improvement was made by using the reaction rate coefficient used in Miller and Bowman [5] for the reaction NH + H ⇌ N + H₂. The rate of this new reaction is higher by a factor of 3, which allows direct reduction of the NH concentration as well as of the NH₂ concentration, to some extent, by shifting the equilibrium. For the highest temperature of 2652 K, the model of Klippenstein et al. [49] predicts a maximum level of NH that is a bit higher than the level predicted by the model from this study and the experimental level. However, the decay in the NH signal is better reproduced by the model of Klippenstein et al. For the lower temperature investigated, 2294 K, the model of Klippenstein et al. is however in better agreement with the data for the maximum of NH predicted. This behavior is similar for other temperatures and NH₃ concentrations, as visible in Fig. 19b. Overall, the model from the present study follows the experimental trend better than the other models, especially compared to the model from Klippenstein et al. which is in close agreement with the data for the lowest temperatures but rapidly deviates from the experimental profile as the temperature increases. The model from the present

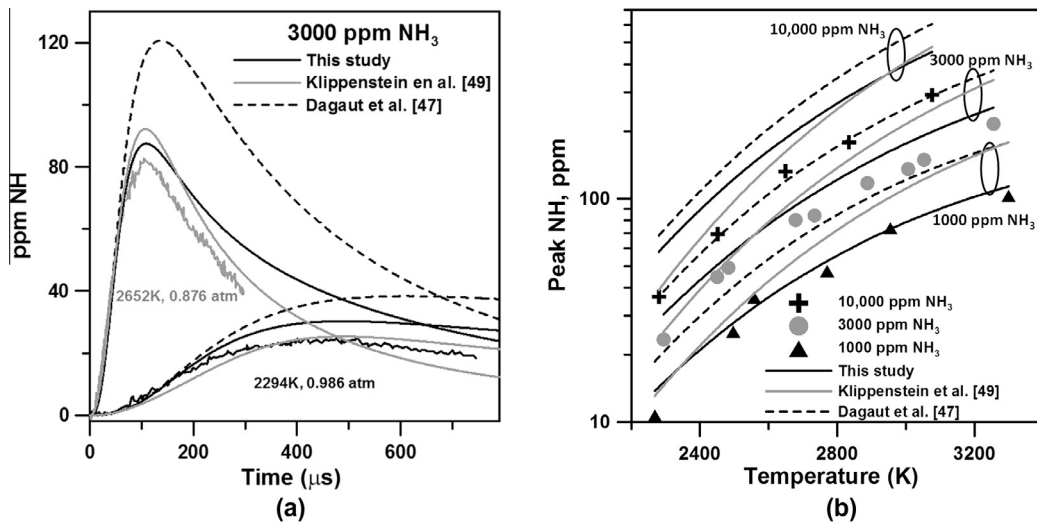


Fig. 19. Comparison between the models and the experiments from Davidson et al. [36] for (a) NH profiles, and (b) maximum NH level for the pyrolysis of diluted mixtures of NH₃ in Ar.

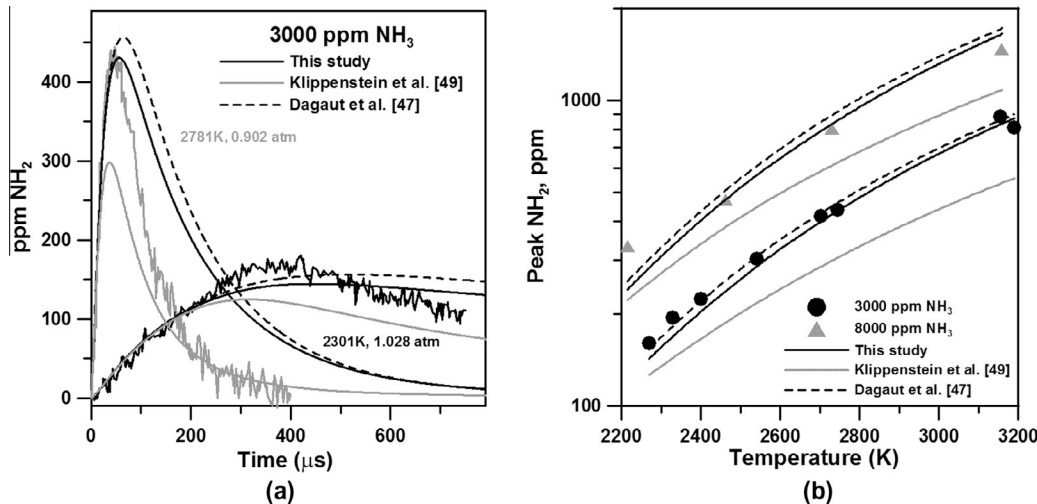


Fig. 20. Comparison between the models and the experiments from Davidson et al. [36] for (a) NH₂ profiles, and (b) maximum NH₂ level for the pyrolysis of diluted mixtures of NH₃ in Ar at various temperatures.

study predicts well the data at an initial NH₃ mole fraction of 0.001 but tends to over-predict the amount of NH formed for higher NH₃ concentrations.

Similar results are available with NH₂ as can be seen in Fig. 20. Profiles for NH₂ (Fig. 20a) are noticeably under-predicted by the mechanism of Klippenstein et al. [49], whereas predictions from the mechanisms of Dagaut et al. [47] and from the present study are close to each other and in relatively good agreement with the data. The maximum NH₂ concentration is well predicted by these two mechanisms over a wide range of temperatures, as can be seen in Fig. 20b.

Finally, the shock-tube data from Drummond [56] were selected to validate the model as N₂O was used as an oxidant instead of O₂, hence validating both N₂O and NH₃ sub-mechanisms at the same time. Although it is not reported that the surface was passivated with NH₃ prior to taking those measurements, the relatively high concentration of NH₃ in the mixture (4 vol.%) should prevent there being too large of a decrease in the initial NH₃ concentration. The modeling pressure was taken at 3.9 atm (the experimental data are reported to be between 3.3 and 4.4 atm) and, as

can be seen in Fig. 21, all the mechanisms are in close agreement with the data, although the predicted activation energy is a bit too low.

To further validate the mechanism, laminar flame speed data with ammonia would have been valuable. It is worth mentioning that although the burning velocity of ammonia-containing mixtures was measured in a few studies in the past [71,72,16], none of these measurements can be considered as accurate due to the lack of corrections of the burning velocity, namely for the effects of flame stretch [20]. It can therefore be concluded that new, accurate measurements for the burning velocity of ammonia are needed.

5. Sensitivity analysis

To further exhibit the difference between the models and to identify important reactions for NH₃ oxidation, a sensitivity analysis on the OH* radical was performed for the experiments with 99% Ar dilution. It has been shown in previous studies by the authors that OH* sensitivity analyses tend to produce results that are very

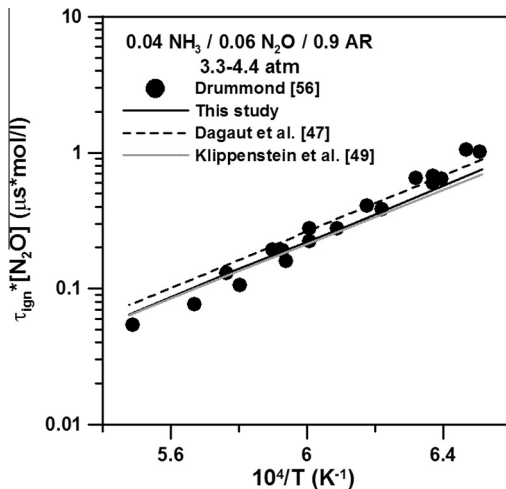


Fig. 21. Comparison between models and experiments from Drummond [56] for the ignition delay times of a 0.04 NH₃/0.06 N₂O mixture diluted in Ar.

similar to those obtained from sensitivity analyses performed with respect to the ignition delay time [60]. Hence, the important reactions from the OH* sensitivity analysis can be assumed to be the important reactions for the ignition process. Figure 22 shows the normalized results of this sensitivity analysis for some selected

conditions: $\phi = 0.5$, 1.4 atm, and 2000 K, where a noticeable difference can be observed between the models in terms of ignition delay time; $\phi = 1.0$, 30 atm, and 1580 K, where the three models yield very similar results; and $\phi = 2.0$, 11 atm, and 2000 K, where the mechanism proposed in this study and the mechanism of Dagaut et al. [47] are close to each other (the mechanism from Klippenstein et al. [49] being more reactive at these conditions).

For the fuel-lean, lower-pressure condition (Fig. 22a–c), the sensitivity analysis shows that the two most-promoting reactions ($\text{NH}_3 + \text{M} \rightleftharpoons \text{NH}_2 + \text{H} + \text{M}$ (r1) and $\text{H} + \text{O}_2 \rightleftharpoons \text{OH} + \text{O}$ (r2)) and the most-inhibiting reaction ($\text{NH}_3 + \text{H} \rightleftharpoons \text{NH}_2 + \text{H}_2$ (r3)) are the same for all 3 models. Differences between the model from Dagaut et al. and the modified version proposed in this study are not large in general. Overall, most of the reactions are the same and rank similarly in terms of relative sensitivity. One noticeable difference is that the most-sensitive reaction $\text{NH}_3 + \text{M} \rightleftharpoons \text{NH}_2 + \text{H} + \text{M}$ (r1) has a more-prominent role in the modified mechanism, the other reactions being normalized to this one. Apart from the three aforementioned reactions, several differences are visible between the model from Klippenstein et al. and the model proposed in the present study, with the role of the N₂H₂ species being very important in the mechanism of Klippenstein et al. The sensitivity study using the mechanisms showed that the N₂Hx (N₂Hx = N₂H₂, N₂H₃, and N₂H₄) chemistry in the model of Klippenstein et al. has a great role in the discrepancy between the results of this model and the data from this study.

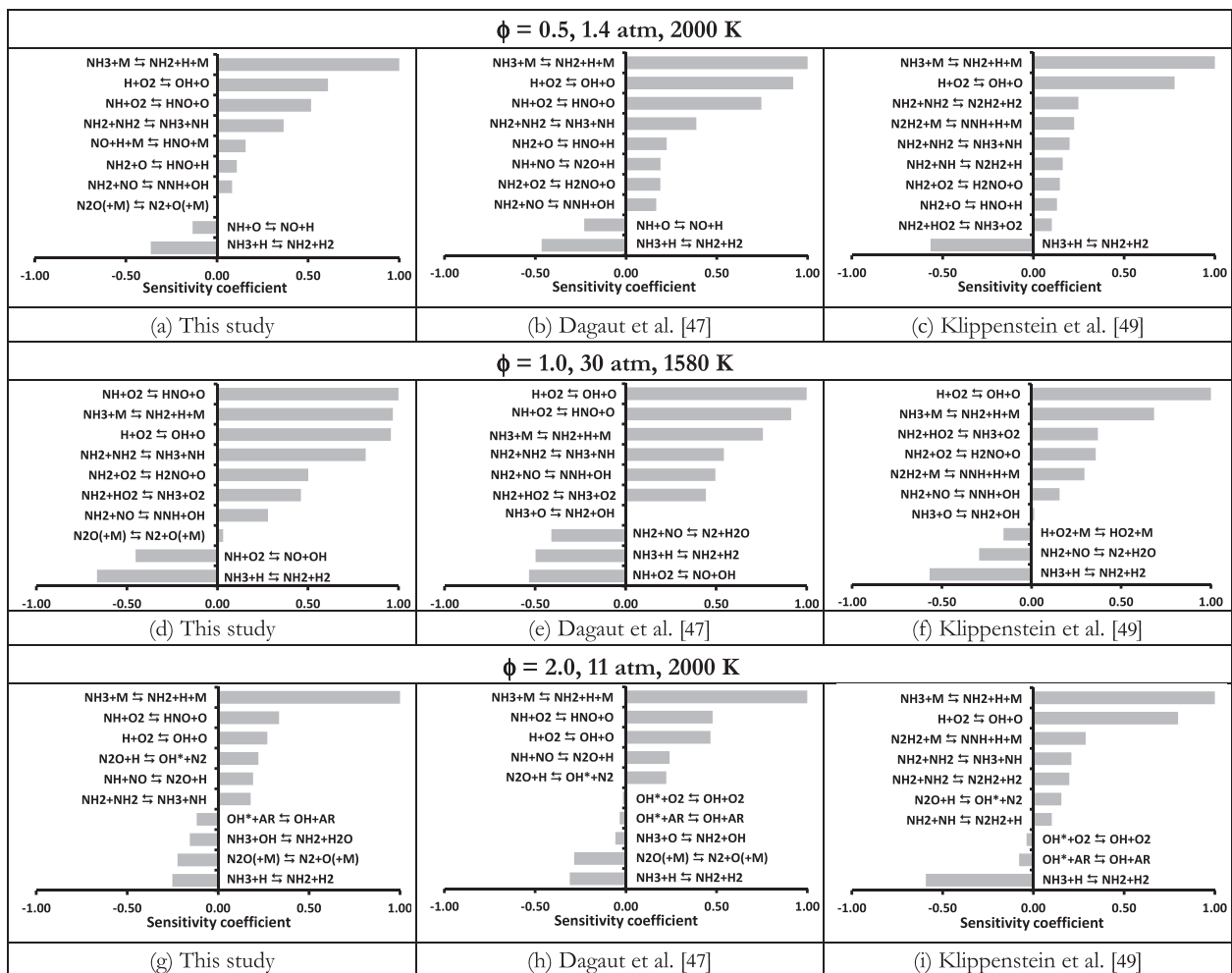


Fig. 22. Normalized sensitivity analysis on OH* for some selected conditions at 99% Ar dilution with the mechanism proposed in this study ((a), (d), and (g)), the mechanism from Dagaut et al. [47] ((b), (e), and (h)), and the mechanism from Klippenstein et al. [49] ((c), (f), and (i)).

For the stoichiometric case at 30 atm, Fig. 22d–f, where the models yield similar results at low temperature (see Fig. 4b), the sensitivity analysis exhibits many differences between the models. The comparison of the results for the model proposed in this study and the model of Dagaut et al. shows that the most-sensitive (promoting and inhibiting) reactions are the same between these two models. However, due to the modifications made during this study, their relative sensitivities (and order relative to the most-sensitive reactions) are different. As for the previous condition, the sensitivity of the reaction $H + O_2 \rightleftharpoons OH + O$ (r2) is reduced in the modified mechanism compared to the reaction (r1) and $NH + O_2 \rightleftharpoons HNO + O$ (r4) (third most-sensitive reaction, but with a high sensitivity coefficient (most sensitive reaction in Dagaut et al. [47])). It is also interesting to note that the reaction $N_2O(+M) \rightleftharpoons N_2 + O(+M)$ (r5) appears in the 10 most-sensitive reactions of the modified mechanism, for all condition in Fig. 22. It therefore stresses the importance of the N_2O sub-mechanism in the ignition chemistry during ammonia oxidation. Once again, most of the sensitive reactions are the same between the mechanism of Klippenstein et al. and the model proposed in this study. In addition to the presence of a reaction involving N_2H_2 , one can notice the presence of the inhibiting reaction $H + O_2 + M \rightleftharpoons HO_2 + M$ (r6), the latest one being not observed with the other models, including with the model proposed in this study with the updated H_2/O_2 chemistry from Kéromnès et al. [64].

For the fuel-rich condition at 10 atm, Fig. 22g–i, the sensitivity analysis shows that the differences between the model of Dagaut et al. and the model proposed in this study are rather slim. In fact, 8 out of 10 reactions are the same or nearly on the same order in terms of normalized sensitivities. The results of this sensitivity analysis hence confirm that the modifications to the model of Dagaut et al. are not very important in regards to the NH_3 chemistry, although predictions were improved for most of the other NOx data, as shown above. At this fuel-rich condition, the difference between the model proposed in the present study and the model of Klippenstein et al. are relatively important. Although the most-sensitive reactions are the same, it is worth mentioning that most of the promoting reactions with an intermediate sensitivity are different. In the case of the model of Klippenstein et al., those intermediate-sensitivity reactions are pyrolysis reactions (i.e. without involvement of either oxygen molecules or atoms) that involve NH_2 or N_2H_2 . This importance of these species illustrates some potentially important differences in the treatment of the NH_3 oxidation between the models and helps explain the difference in terms of predictions for the new ignition delay time measurements presented in this study.

6. Conclusions

It is important to understand the details of NH_3 combustion chemistry for practical reasons such as the control of NOx formation or for NOx removal processes. To date, several shock-tube studies have been performed over the past few decades, and several detailed kinetics mechanisms are available from the literature. Unfortunately, experimental conditions are not clearly reported in the shock-tube literature, and large discrepancies are observed amongst the models compared herein, making the selection of a good core model to predict NH_3 combustion difficult. Thus, new and reliable ignition delay time measurements were obtained over a wide range of conditions (around 1.4, 11, and 30 atm, between 1560 and 2490 K, and for equivalence ratios 0.5, 1.0, and 2.0). Results showed that both the equivalence ratio and the pressure had important effects on the ignition delay time of ammonia.

Models from the literature were then compared to this new set of data, and it was found that only the model from Dagaut et al.

[47] provided satisfactory results (when the reaction $N_2O + H \rightleftharpoons N_2 + OH^*$ from Hidaka et al. [58] was added with the OH^* mechanism from Hall and Petersen [54]). This mechanism was further improved using sub-mechanisms and reactions available in the literature, and the final NOx mechanism is able to predict selected $NH_3/HCN/NO_2$ and N_2O data with good accuracy over a range of conditions and types of experiment. The sensitivity analysis showed that the differences between the initial model of Dagaut et al. and the model proposed in this study are rather slim for NH_3 oxidation, although significant improvements were made on the modeling of NOx/ N_2O data. Some noticeable differences were however observed between the most-recent literature model from Klippenstein et al. [49] and the final model of the present study, notably for fuel-rich conditions where pyrolysis reactions involving NH_2 and N_2H_2 have a greater role in the most-recent mechanism.

Acknowledgments

This material is based upon the work supported by two UTSR grants from the Department of Energy, NETL, under Award Numbers DE-FE0004679 and DE-FE0011778.

References

- [1] S. Sukumaran, S.-C. Kong, Combust. Flame 160 (2013) 2159–2168.
- [2] D. Xu, D.R. Tree, R.S. Lewis, Biomass Bioenergy 35 (2011) 2690–2696.
- [3] T. Mendiara, P. Glarborg, Combust. Flame 156 (2009) 1937–1949.
- [4] K. Kohse-Höninghaus, D.F. Davidson, A.Y. Chang, R.K. Hanson, J. Quant. Spectrosc. Radiat. Transfer 42 (1989) 1–17.
- [5] J.A. Miller, C.T. Bowman, Prog. Energy Combust. Sci. 15 (1989) 287–338.
- [6] P. Glarborg, A.D. Jensen, J.E. Johnson, Prog. Energy Combust. Sci. 29 (2003) 89–113.
- [7] S. Salimian, R.K. Hanson, C.H. Kruger, Combust. Flame 56 (1984) 83–95.
- [8] J.A. Miller, P. Glarborg, Int. J. Chem. Kinet. 31 (1999) 757–765.
- [9] C.C. Schmidt, C.T. Bowman, Combust. Flame 127 (2001) 1958–1970.
- [10] J.A. Miller, M.J. Pilling, J. Troe, Proc. Combust. Inst. 30 (2005) 43–88.
- [11] D.T. Pratt, E.S. Starkman, Proc. Combust. Inst. 12 (1969) 891–899.
- [12] C. Duynslaeger, F. Contino, J. Vandooren, H. Jeanmart, Combust. Flame 159 (2012) 2799–2805.
- [13] L. Cohen, Fuel 34 (1955) 123–127.
- [14] C.P. Fenimore, G.W. Jones, J. Phys. Chem. 65 (1961) 298–303.
- [15] D.I. MacLean, H.G. Wagner, Proc. Combust. Inst. 11 (1967) 871–878.
- [16] V. Zakaznov, L. Kursheva, Zh. Prikl. Khim. 53 (1980) 1865–1867.
- [17] C.J. Dasch, R.J. Blint, Combust. Sci. Technol. 41 (1984) 223–244.
- [18] A.M. Dean, M.-S. Chou, D. Stern, Int. J. Chem. Kinet. 16 (1984) 633–653.
- [19] J. Bian, J. Vandooren, P.J. van Tiggelen, Proc. Combust. Inst. 21 (1986) 953–963.
- [20] M. Brown, D. Smith, Proc. Combust. Inst. 25 (1994) 1011–1018.
- [21] C. Duynslaeger, H. Jeanmart, J. Vandooren, Proc. Combust. Inst. 32 (2009) 1277–1284.
- [22] T. Takeyama, H. Miyama, J. Chem. Phys. 42 (1965) 3737–3738.
- [23] T. Takeyama, H. Miyama, Bull. Chem. Soc. Jpn. 38 (1965) 1670–1674.
- [24] T. Takeyama, H. Miyama, Bull. Chem. Soc. Jpn. 39 (1966) 2352–2355.
- [25] T. Takeyama, H. Miyama, Bull. Chem. Soc. Jpn. 39 (1966) 2609–2612.
- [26] T. Takeyama, H. Miyama, Proc. Combust. Inst. 11 (1967) 845–852.
- [27] H. Miyama, R. Endoh, Combust. Flame 11 (1967) 359–360.
- [28] H. Miyama, R. Endoh, J. Chem. Phys. 46 (1967) 2011–2012.
- [29] D.C. Bull, Combust. Flame 12 (1968) 603–610.
- [30] H. Miyama, Bull. Chem. Soc. Jpn. 41 (1968) 1761–1765.
- [31] H. Miyama, J. Chem. Phys. 48 (1968) 1421–1422.
- [32] J.N. Bradley, R.N. Butlin, D. Lewis, Trans. Faraday Soc. 64 (1968) 71–78.
- [33] L.J. Drummond, Combust. Sci. Technol. 5 (1972) 175–182.
- [34] N. Fujii, H. Miyama, M. Koshii, T. Asaba, Proc. Combust. Inst. 18 (1981) 873–883.
- [35] S. Salimian, R.K. Hanson, C.H. Kruger, Int. J. Chem. Kinet. 16 (1984) 725–739.
- [36] D.F. Davidson, K. Kohse-Höninghaus, A.Y. Chang, R.K. Hanson, Int. J. Chem. Kinet. 22 (1990) 513–535.
- [37] A.M. Dean, J.E. Hardy, R.K. Lyon, Proc. Combust. Inst. 19 (1982) 97–105.
- [38] T. Hulgard, K. Dam-Johansen, AIChE J. 39 (1993) 1342–1354.
- [39] T. Hasegawa, M. Sato, Combust. Flame 114 (1998) 246–258.
- [40] V.J. Wargadalam, G. Löffler, F. Winter, H. Hofbauer, Combust. Flame 120 (2000) 465–478.
- [41] A. Konnov, J. De Ruyck, Combust. Sci. Technol. 168 (2001) 1–46.
- [42] Ø. Skreiberg, P. Kilpinen, P. Glarborg, Combust. Flame 136 (2004) 501–518.
- [43] J. Bian, J. Vandooren, P. van Tiggelen, Proc. Combust. Inst. 23 (1990) 379–386.
- [44] M.A. Mueller, R. Yetter, F. Dryer, Int. J. Chem. Kinet. 32 (2000) 317–339.
- [45] K.J. Hughes, A.S. Tomlin, E. Hampartsoumian, W. Nimmo, I.G. Zsély, M. Ujvári, T. Turányi, A.R. Clague, M.J. Pilling, Combust. Flame 124 (2001) 573–589.

- [46] P. Dagaut, A. Nicolle, Proc. Combust. Inst. 30 (2005) 1211–1218.
- [47] P. Dagaut, P. Glarborg, M.U. Alzueta, Prog. Energy Combust. Sci. 34 (2008) 1–46.
- [48] R. Mével, S. Javoy, F. Lafosse, N. Chaumeix, G. Dupré, C.-E. Paillard, Proc. Combust. Inst. 32 (2009) 359–366.
- [49] S.J. Klippenstein, L.B. Harding, P. Glarborg, J.A. Miller, Combust. Flame 158 (2011) 774–789.
- [50] T. Mendiara, P. Glarborg, Combust. Flame 156 (2009) 1937–1949.
- [51] C.J. Aul, W.K. Metcalfe, S.M. Burke, H.J. Curran, E.L. Petersen, Combust. Flame 160 (2013) 1153–1167.
- [52] E.L. Petersen, M.J.A. Rickard, M.W. Crofton, E.D. Abbey, M.J. Traum, D.M. Kalitan, Meas. Sci. Technol. 16 (2005) 1716–1729.
- [53] T.R. Roose, R.K. Hanson, C.H. Kruger, Proc. Combust. Inst. 18 (1981) 854–862.
- [54] J.M. Hall, E.L. Petersen, Int. J. Chem. Kinet. 38 (2006) 714–724.
- [55] Y. Hidaka, H. Takuma, M. Suga, J. Phys. Chem. 89 (1985) 4903–4905.
- [56] L. Drummond, Aust. J. Chem. 20 (1967) 2331–2341.
- [57] O. Mathieu, A. Levacque, E.L. Petersen, Int. J. Hydrogen Energy 37 (2012) 15393–15405.
- [58] Y. Hidaka, H. Takuma, M. Suga, Bull. Chem. Soc. Jpn. 58 (1985) 2911–2916.
- [59] M. Kopp, M. Brower, O. Mathieu, E.L. Petersen, F. Güthe, Appl. Phys. B 107 (2012) 529–538.
- [60] O. Mathieu, A. Levacque, E.L. Petersen, Proc. Combust. Inst. 34 (2013) 633–640.
- [61] G. Dayma, P. Dagaut, Combust. Sci. Technol. 178 (2006) 1999–2024.
- [62] T. Higashihara, K. Saito, I. Murakami, J. Phys. Chem. 87 (1983) 3707–3712.
- [63] K. Thielen, P. Roth, Combust. Flame 69 (1987) 141–154.
- [64] A. Kéromnès, W.K. Metcalfe, K.A. Heufer, N. Donohoe, A.K. Das, C.-J. Sung, J. Herzler, C. Naumann, P. Griebel, O. Mathieu, M.C. Krejci, E.L. Petersen, W.J. Pitz, H.J. Curran, Combust. Flame 160 (2013) 995–1011.
- [65] D.L. Baulch, C.T. Bowman, C.J. Cobos, R.A. Cox, T. Just, J.A. Kerr, et al., J. Phys. Chem. Ref. Data 34 (2005) 757–1397.
- [66] A.A. Konnov, Combust. Flame 156 (2009) 2093–2105.
- [67] R. Sivaramakrishnan, K. Brezinsky, G. Dayma, P. Dagaut, Phys. Chem. Chem. Phys. 9 (2007) 4230–4244.
- [68] J. Parks, N.D. Giles, J. Moore, M.C. Lin, J. Phys. Chem. A 102 (1998) 10099–10105.
- [69] A.E. Lutz, R.J. Kee, J.A. Miller, Senkin: a fortran program for predicting homogeneous gas phase chemical kinetics with sensitivity analysis, Report SAND87-8248, Sandia National Laboratories, 1988.
- [70] P. Glarborg, R.J. Kee, J.F. Grcar, J.A. Miller, PSR: a Fortran program for modeling well-stirred reactors, Report SAND86-8209, Sandia National Laboratories, 1986
- [71] P. Ausloos, A. van Tiggelen, Bull. Soc. Chim. Belg. 6 (1951) 433–445.
- [72] D.G.R. Andrews, P. Gray, Combust. Flame 8 (1964) 113–126.